Theoretical Model for Insertion of the 16-Electron Species (η^5-C_5H_5)M(L) into Saturated Hydrocarbons. A (η^5-C_5H_5)M(CO) + CH_4 (M = Ru^-, Os^-, Rh, Ir, Pd^+, Pt^+) Case Study

Ming-Der Su* and San-Yan Chu*

Department of Chemistry, National Tsing Hua University, Hsinchu 30043, Taiwan, ROC

Received October 1, 1996[⊗]

The potential energy surfaces corresponding to the reaction of the 16-electron (η^5-C_5R_5)M(CO) (M = Ru^-, Os^-, Rh, Ir, Pd^+, Pt^+) with methane have been investigated by employing the MP2, MP4SDTQ, and B3LYP levels of theory. It is found that a more electron-rich as well as heavier transition-metal center (i.e., the third row) will facilitate the oxidative-addition reactions with alkane C−H bonds. In contrast, a very electron-deficient and a lighter transition metal center (i.e., the second row) will tend to undergo reductive-elimination reactions of C−H bond forming. A comparison of MP2, MP4, and density functional theory in the CpM(CO) model systems shows that the B3LYP method is able to avoid the multireference problems that ab initio methods have. Nevertheless, the MP2/LANL1DZ method can provide qualitatively correct results.

I. Introduction

One of the most beneficial features of transition-metal complexes is their ability to "activate" carbon−hydrogen bonds in completely saturated organic compounds. This has attracted considerable interest over the last decade.[1] Particularly, it has been shown that [(η^5-C_5R_5)M(PMe_3)-H_2] (M = Rh, Ir) and [(η^5-C_5R_5)Ir($CO)_2$] (R = H, Me) complexes undergo intermolecular oxidative addition to C−H bonds of arenes and alkanes under relatively mild conditions via a photochemical route.[2] Several theoretical studies have confirmed the low activation barrier in the case of CpM(CO) (Cp = η^5-C_5H_5; M = Rh, Ir).[3] However, no previous ab initio study has to our knowledge been published on the dependence in the reaction of barrier height as a function of the nature of the transition-metal center. In this work, we have therefore chosen the CpM(CO) (M = Ru^-, Os^-, Rh, Ir, Pd^+, Pt^+) intermediates as models to reveal their mechanisms and the reactivities of the oxidative addition to the C−H bond of CH_4. Moreover, in order to compare the optimized geometries as well as their energetics, we have now used two kinds of theories in the present study, i.e., the ab initio method and the density functional theory (DFT) (vide infra).

II. Computational Methods

Theoretical calculations presented here were carried out using the GAUSSIAN94 program.[4] All equilibrium geometries and transition structures were fully optimized without any symmetry constraints using the second-order Møller−Plesset perturbation (MP2) theory[5] with LANL1DZ basis set (MP2/LANL1DZ). For better energetics, the electron correlation effect was taken into account with the fourth-order MP level including single, double, triple, and quadruple excitations (MP4SDTQ) at the MP2-optimized structures (MP4SDTQ//MP2/LANL1DZ).[5]

Also, all geometries were fully optimized by employing DFT. For DFT calculations, the hybrid gradient-corrected exchange functional proposed by Becke[6ab] was combined with the gradient-corrected correlation functional of Lee, Yang, and Parr.[6c] Henceforth, we will denote this functional as B3LYP, which has been shown to be quite reliable both in geometry and in energies for semiquantitative discussions.[7] In addition, in previous works, we and other researchers have found the LANL2DZ basis set accurate and reliable in describing the electronic and structural properties pertaining to a variety of complexes.[8] Hence, the B3LYP calculation is denoted by B3LYP/LANL2DZ.

The LANL1DZ and LANL2DZ basis sets contain pseudopotentials for core electrons and a double-ζ basis set for valence electrons.[9] The LANL2DZ basis differs from the LANL1DZ

[⊗] Abstract published in *Advance ACS Abstracts,* March 1, 1997.

(1) For reviews, see: (a) Hill, C. L. *Activation and Functionalization of Alkanes*; Wiley: New York, 1989. (b) Davies, J. A.; Watson, P. L.; Liebman, J. F.; Greenberg, A. *Selective Hydrocarbon Activation: Principles and Progress*; VCH: New York, 1990. (c) Crabtree, R. H. *Angew. Chem., Int. Ed. Engl.* **1993**, *32*, 789.

(2) (a) Janowicz, A. H.; Bergman, R. G. *J. Am. Chem. Soc.* **1983**, *105*, 3929. (b) Janowicz, A. H.; Perima, R. A.; Buchanan, J. M.; Kovac, C. A.; Struker, J. M.; Wax, M. J.; Bergman, R. G. *Pure Appl. Chem.* **1984**, *56*, 13 and references cited therein. (c) Jones, W. D.; Feher, F. J. *J. Am. Chem. Soc.* **1984**, *106*, 1650. (d) Bergman, R. G. *Science* **1984**, *223*, 902. (e) Wasserman, E. P.; Moore, C. B.; Bergman, R. G. *Science* **1992**, *255*, 315 and references cited therein.

(3) (a) Ziegler, T.; Tschinke, V.; Fan, L.; Becke, A. D. *J. Am. Chem. Soc.* **1989**, *111*, 9177. (b) Song, J.; Hall, M. B. *Organometallics* **1993**, *12*, 3118. (c) Musaev, D. G.; Morokuma, K. *J. Am. Chem. Soc.* **1995**, *117*, 799. (d) Siegbahn, P. E. M. *J. Am. Chem. Soc.* **1996**, *118*, 1487. (e) Couty, M.; Bayse, C. A.; Jimenez-Catano, R.; Hall, M. B. *J. Phys. Chem.* **1996**, *100*, 13976. (f) Su, M.-D.; Chu, S.-Y., submitted for publication.

(4) Gaussian 94, Revision B.2: M. J. Frisch, G. W. Trucks, H. B. Schlegel, P. M. W. Gill, B. G. Johnson, M. A. Robb, J. R. Cheeseman, T. Keith, G. A. Petersson, J. A. Montgomery, K. Raghavachari, M. A. Al-Laham, V. G. Zakrzewski, J. V. Ortiz, J. B. Foresman, J. Cioslowski, B. B. Stefanov, A. Nanayakkara, M. Challacombe, C. Y. Peng, P. Y. Ayala, W. Chen, M. W. Wong, J. L. Andres, E. S. Replogle, R. Gomperts, R. L. Martin, D. J. Fox, J. S. Binkley, D. J. Defrees, J. Baker, J. P. Stewart, M. Head-Gordon, C. Gonzalez, and J. A. Pople, Gaussian, Inc., Pittsburgh PA, 1995.

(5) Hehre, W. J.; Random, L.; Schleyer, P. v. R.; Pople, J. A. *Ab-initio Molecular Orbital Theory*; Wiley-Interscience: New York, 1986, and references therein.

(6) (a) Becke, A. D. *Phys. Rev. A* **1988**, *38*, 3098. (b) Becke, A. D. *J. Chem. Phys.* **1993**, *98*, 5648. (c) Lee, C.; Yang, W.; Parr, R. G. *Phys. Rev. B* **1988**, *37*, 785.

(7) (a) Stevens, P. J.; Devlin, F. J.; Chablowski, C. F.; Frisch, M. J. *J. Phys. Chem.* **1994**, *98*, 11623. (b) Ricca, A.; Bauschlicher, C. W. *Theor. Chim. Acta* **1995**, *92*, 123.

(8) (a) Gugelchuk, M. M. *J. Mol. Struct. (THEOCHEM)* **1995**, *357*, 263. (b) Su, M.-D., Chu, S.-Y., submitted for publication.

S0276-7333(96)00837-0 CCC: $14.00

basis by inclusion of the $(n-1)$s and $(n-1)$p electrons in the valence space of the transition-metal atom. The standard double-ζ basis sets were chosen for the hydrogen, carbon, and oxygen atoms.[10] Frequency calculations were carried out on the optimized geometries at the MP2/LANL1DZ and B3LYP/LANL2DZ levels of theory to characterize the true nature of the stationary points obtained in the optimization process.

III. General Considerations

In this section, we shall analyze the electronic structures of the CpM(CO)·CH_4 systems by interacting CpM(CO) and CH_4 fragments. The frontier orbitals of the 16-electron CpM(CO) fragment are known[11] and are shown in **1**. A block of three occupied levels, 1a′(x^2-y^2), 1a″(xy), and 2a′(z^2), are at low energy, which are primarily made up of metal d orbitals. In the somewhat higher occupied level (2a″), the metal d_{xz} orbital is hybridized with metal p_y and d_{xy} orbitals in such a way that orbital lobes point toward the missing ligand of a parent $CpML_2$ molecule. The lowest unoccupied molecular orbital (LUMO) is 3a′, a hybrid of metal d_{yz}, s, and p_z orbitals as indicated in **2**. Note that it is the two frontier levels 2a″ and 3a′ that allow one to view 16-electron CpML species as organometallic analogues of CH_2.[12]

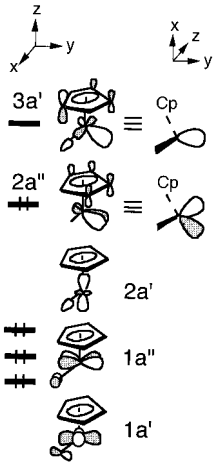

1

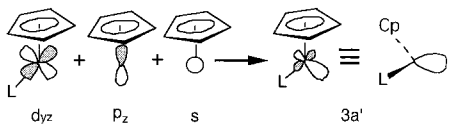

2

On the other hand, in a canonical MO description of a hydrocarbon, there are no isolated MOs that describe a particular C−H σ bond. For example, in methane there is a lower lying $2A_1$ orbital and three degenerate T_2 orbitals.[13] In a tetrahedral array, both hydrogens (or carbons) directly bound to the sp^3 carbon occupy a common plane, and they are related by symmetry and may comprise an orbital with σ symmetry (σ_{CH_2}) as in **3** or a π_{CH_2} orbital as in **4**.[14] Therefore, we prefer to use a canonical MO rather than make a localized description of the C−H bond, since it is easier to visualize the coalescence of the electron donor and acceptor when the approximate axis of the reaction is clearly defined (vide infra).

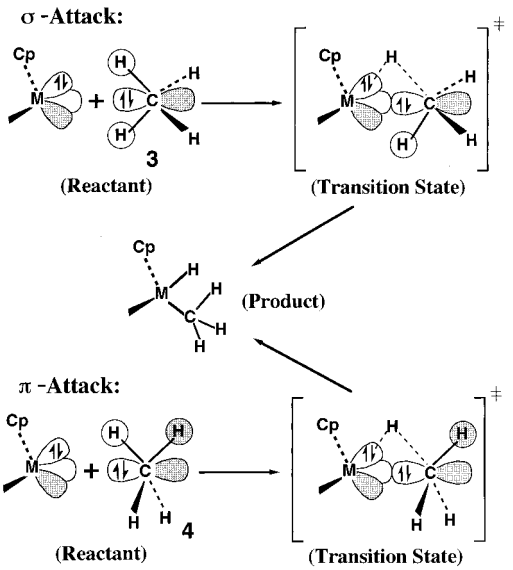

Figure 1. Insertion of 16-electron CpM(CO) into hydrocarbons along a σ_{CH_2} path, where the empty CpM(CO) s/p/d orbital is aligned with the carbon p orbital of a σ_{CH_2} fragment orbital, or along a π_{CH_2} path, where the CpM(CO) s/p/d orbital is aligned with a π_{CH_2} fragment orbital.

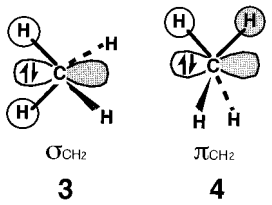

Hence, in this qualitative theoretical treatment, we identify the CpML fragment as having an empty electrophilic orbital (i.e., 3a′ as shown in **1**) that can interact with either the doubly occupied σ_{CH_2} or the doubly occupied π_{CH_2} fragment orbital in methane to arrive at the transition state. The CpML complex may approach methane from two unique directions, as illustrated in Figure 1. For the σ-attack, the empty 3a′ orbital of CpML overlaps with the filled σ_{CH_2} orbital of methane and a 1,2-hydrogen migration takes place in concert with C−M bond formation. Similarly, the π attack proceeds by attack of a filled π_{CH_2} fragment orbital along the axis of the empty 3a′ orbital of CpML with a concerted hydrogen migration into the CpML lone pair (2a″). As a result, the net molecular event involved in the insertion of a CpML complex into a C−H σ bond is the formation of a new metal−carbon σ bond as well as a new metal−hydrogen σ bond, accompanied by the breaking of the C−H σ bond. This is a typical example for the oxidative-addition reaction of a transition-metal

(9) (a) Hay, J. P.; Wadt, W. R. *J. Chem. Phys.* **1985**, *82*, 270. (b) *Ibid.* **1985**, *82*, 284. (c) *Ibid.* **1985**, *82*, 299.

(10) Dunning, T. H.; Hay, P. J. In *Modern Theoretical Chemistry*; Schaefer, H. F., Ed.; Plenum: New York, 1976; pp 1−28.

(11) Hoffmann, P.; Radmanabhan, M. *Organometallics* **1983**, *2*, 1273.

(12) Hoffmann, R. *Angew. Chem., Int. Ed. Engl.* **1982**, *21*, 711.

(13) (a) Bach, R. D.; Andres, J. L.; Su, M.-D.; McDouall, J. J. W. *J. Am. Chem. Soc.* **1993**, *115*, 5768. (b) Bach, R. D.; Su, M.-D.; Aldabagh, E.; Andres, J. L.; Schlegel, H. B. *J. Am. Chem. Soc.* **1993**, *115*, 10237. (c) Bach, R. D.; Su, M.-D. *J. Am. Chem. Soc.* **1994**, *116*, 10103.

(14) In this work, we shall use the σ/π nomenclature[13] to describe the reaction trajectory and define the axis of attack of the valence orbital on the central metal.

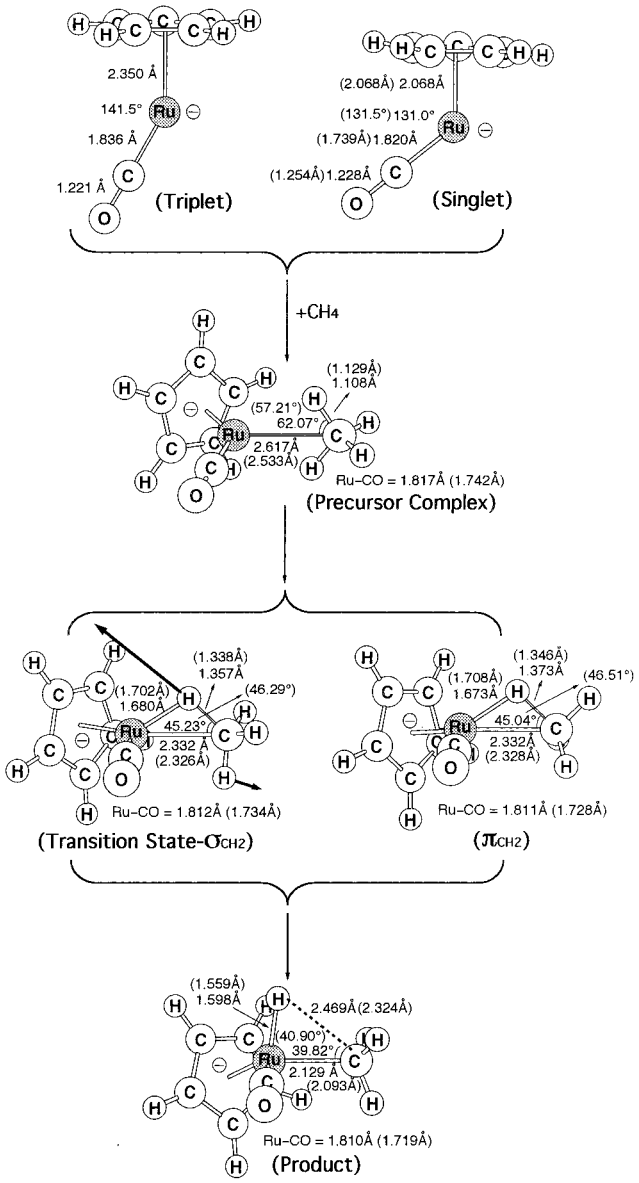

Figure 2. B3LYP/LANL2DZ optimized geometries for the reactants (singlet and triplet), precursor complexes, transition states, and products of [CpRu(CO)]$^-$. The heavy arrows indicate transition vectors for the single imaginary frequency. The MP2/LANL1DZ structures are shown in parentheses (see text).

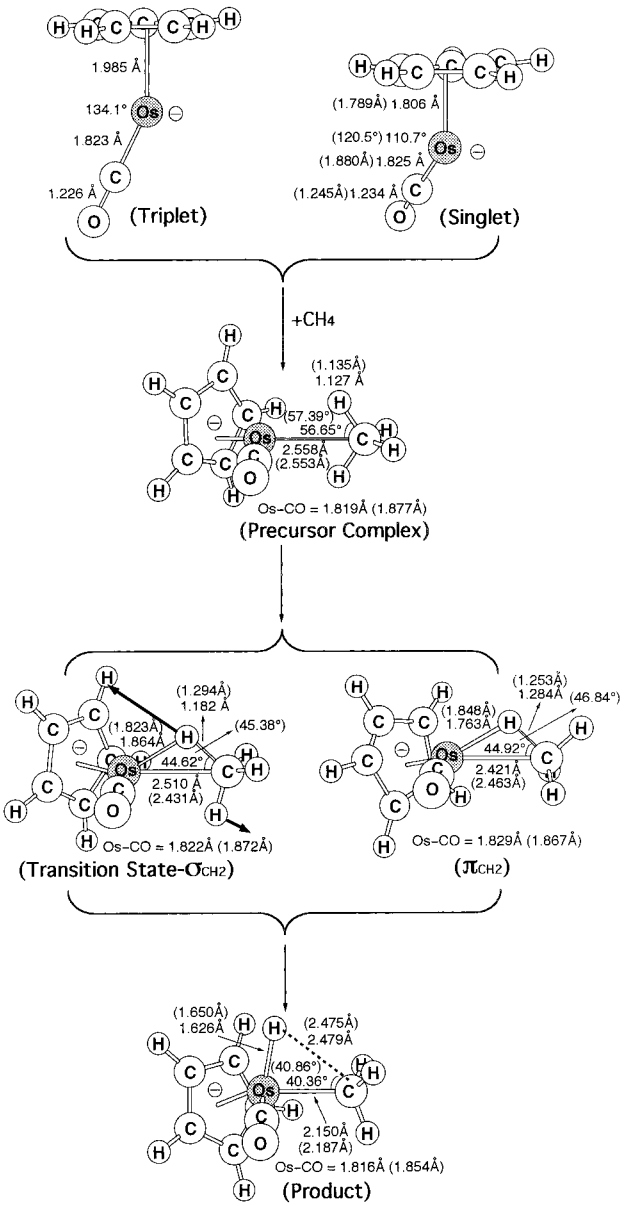

Figure 3. B3LYP/LANL2DZ optimized geometries for the reactants (singlet and triplet), precursor complexes, transition states, and products of [CpOs(CO)]$^-$. The heavy arrows indicate transition vectors for the single imaginary frequency. The MP2/LANL1DZ structures are shown in parentheses (see text).

complex into the C−H bond.[1] In addition, since the experimental evidence suggests that radical intermediates were not involved in the C−H activation reaction for the d^8-CpML (M = Rh, Ir) systems,[2c] it is therefore reasonable to conclude that the mechanism depicted in Figure 1 should be the most likely pathway for Ru, Os, Pd, and Pt analogs (vide infra). Moreover, comparing the σ attack and the π attack in Figure 1, one may anticipate that the CpML insertion in the σ_{CH_2} orientation has fewer steric interactions than a π_{CH_2} approach and provides the insertion product in its staggered lower energy conformation. We shall see the calculational results supporting these predictions below.

IV. Results and Discussion

The fully optimized geometries of the reactants, precursor complexes, transition states, and products for CpM(CO) (M = Ru$^-$, Os$^-$, Rh, Ir, Pd$^+$, Pt$^+$) at the MP2/LANL1DZ and B3LYP/LANL2DZ levels are given in Figures 2−7, respectively. Their energy parameters are listed in Table 1.

Three points are noteworthy. First, as seen in **1**, in the triplet state one electron is situated in the 3a′ orbital, in which antibonding interactions exist between the metal and the ligand as well as the Cp ring, whereas this orbital is empty in the singlet state. It is therefore expected that the distance r(M−X) between the metal atom and the center (X) of the Cp ring, the distance r(M−L), and the angle ∠X−M−L should be larger for the triplet compared to the singlet. This is exactly what we observed in DFT results in Figures 2−7.

Second, according to our DFT calculations in Table 1, it is intriguing to find that the ground states of the [CpRh(CO)], [CpPd(CO)]$^+$, and [CpPt(CO)]$^+$ fragments are singlets, whereas other complexes are triplets. This implies that a complex with the triplet ground state

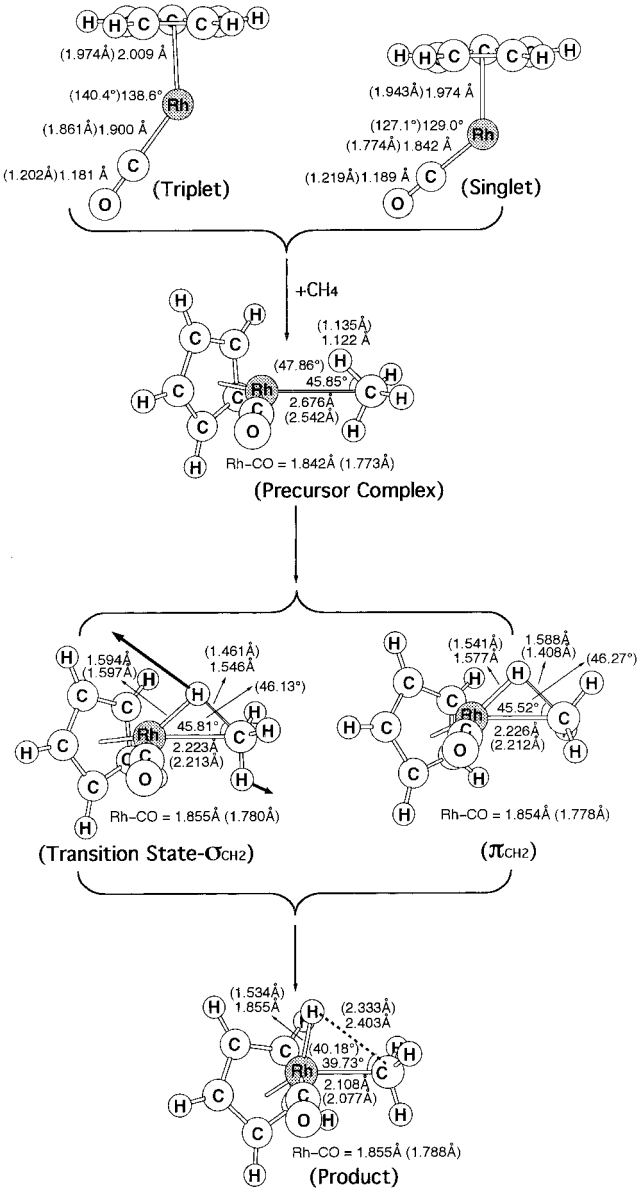

Figure 4. B3LYP/LANL2DZ optimized geometries for the reactants (singlet and triplet), precursor complexes, transition states, and products of [CpRh(CO)]. The heavy arrows indicate transition vectors for the single imaginary frequency. The MP2/LANL1DZ structures are shown in parentheses (see text).

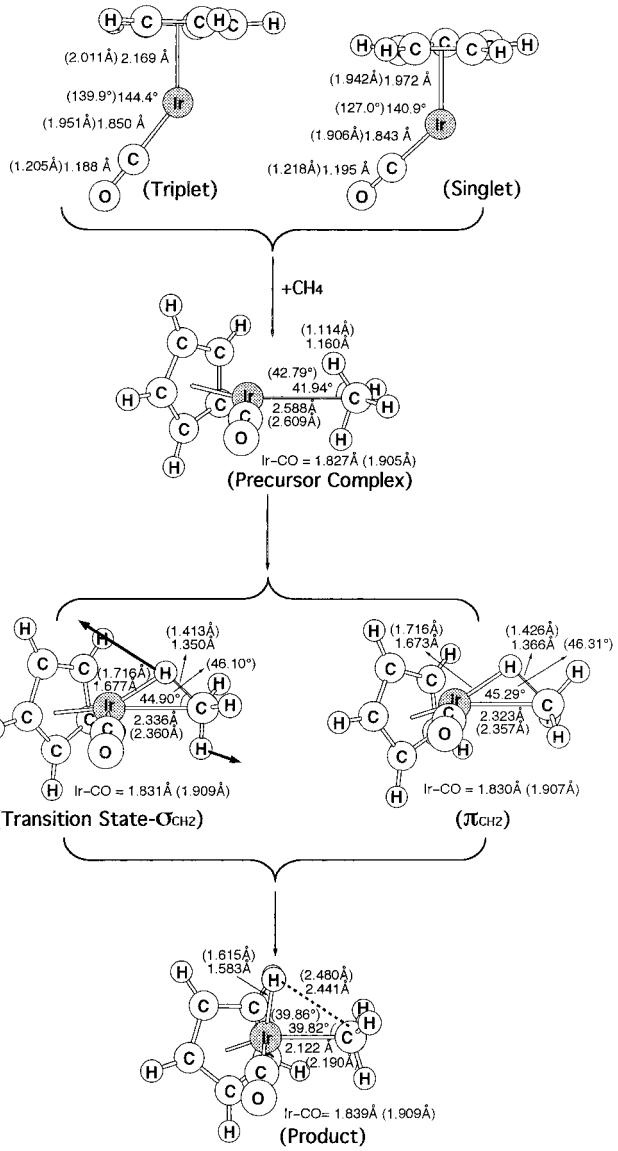

Figure 5. B3LYP/LANL2DZ optimized geometries for the reactants (singlet and triplet), precursor complexes, transition states, and products of [CpIr(CO)]. The heavy arrows indicate transition vectors for the single imaginary frequency. The MP2/LANL1DZ structures are shown in parentheses (see text).

might insert into the saturated C−H bond via a diradical type of mechanism. Nevertheless, it has been well-established that whenever a reactant contains a heavy-atom center which is not necessarily directly involved in the reaction, a strong spin−orbit coupling (SOC) may obtain.[15] In other words, a triplet reactant, via the agency of the heavy atom, can provide a spin-inversion process for transferring to the singlet reactant and then undergoing the singlet reaction. Additionally, our DFT results in Table 1 also suggested that those CpM(CO) (M = Ru^-, Os^-, Ir) fragments with the triplet ground state would have small excitation energy to the first singlet state; i.e., $\Delta E_{st} = -14 - -4.0$ kcal/mol. Thus, due to the fact that CpM(CO) (M = Ru^-, Os^-, Ir) has a small singlet−triplet splitting ΔE_{st} and a heavier transition metal is involved, the SOC is expected to be substantial in those oxidative additions and would wash out differentials based on singlet, triplet distinctions. Moreover, as mentioned previously, no radical components have been detected experimentally in the oxidative-addition reactions of the 16-electron CpML (M = Rh, Ir) systems. For these reasons, it could well be that our concern about the possible *presence* of reactive singlets and triplets is unnecessary.

Third, the three-centered cyclic transition states involving the metal center and carbon and hydrogen atoms undergoing bond cleavage, as expected from the earlier discussions, were observed for 16-electron CpM(CO) complexes at the various metals (M = Ru^-, Os^-, Rh, Ir, Pd^+, Pt^+). It is worth mentioning that in the B3LYP/LANL2DZ calculations only the σ_{CH_2} approach as demonstrated in Figure 1 can lead to the true transition state and the π_{CH_2} approach results in a second-order saddle point possessing two imaginary

(15) (a) Su, M.-D. *Chem. Phys. Lett.* **1995**, *237*, 317. (b) Su, M.-D. *J. Org. Chem.* **1995**, *60*, 6621. (c) Su, M.-D. *J. Phys. Chem.* **1996**, *100*, 4339. (d) Su, M.-D. *Chem. Phys.* **1996**, *205*, 277. (d) Su, M.-D. *J. Org. Chem.* **1996**, *61*, 3080.

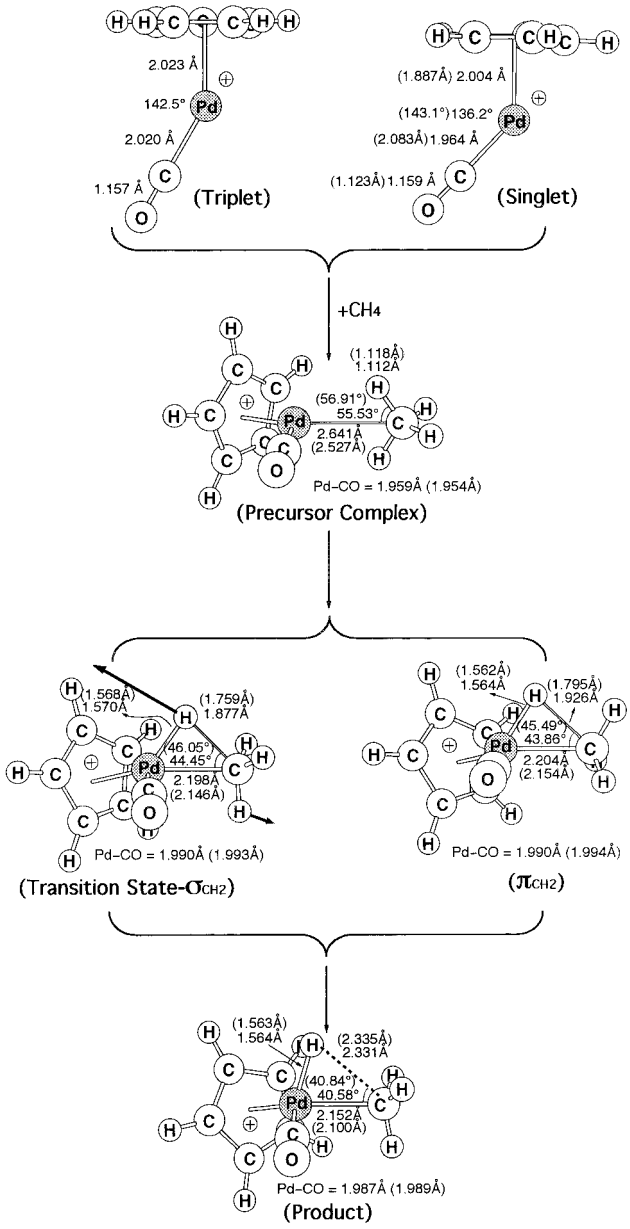

Figure 6. B3LYP/LANL2DZ optimized geometries for the reactants (singlet and triplet), precursor complexes, transition states, and products of $[CpPd(CO)]^+$. The heavy arrows indicate transition vectors for the single imaginary frequency. The MP2/LANL1DZ structures are shown in parentheses (see text).

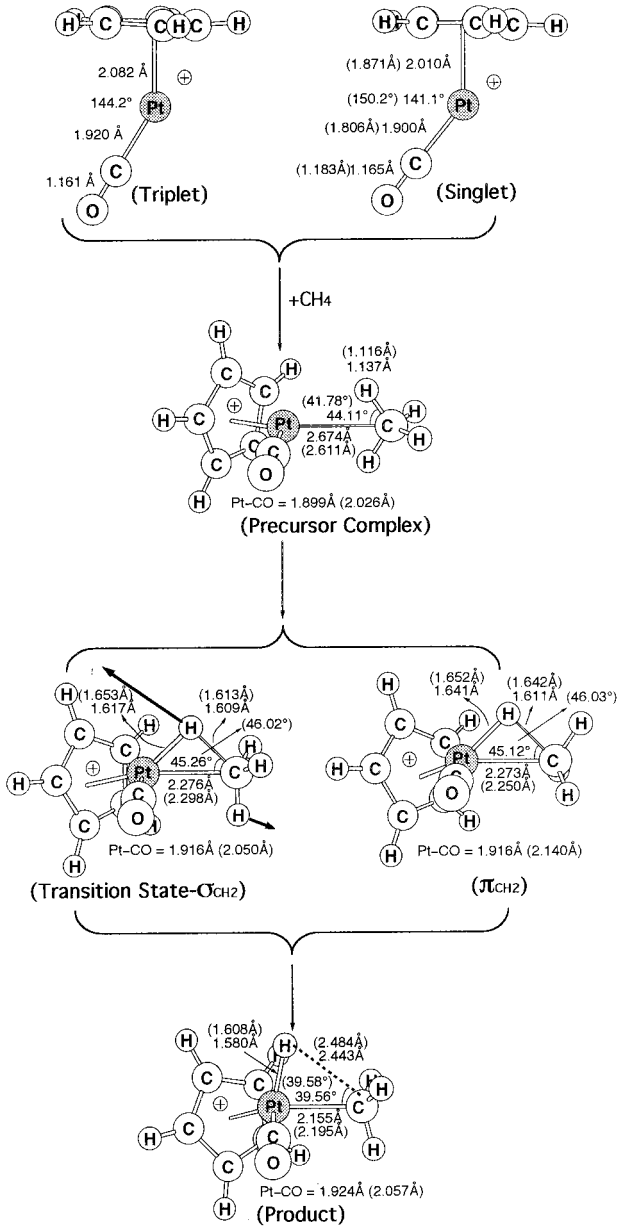

Figure 7. B3LYP/LANL2DZ optimized geometries for the reactants (singlet and triplet), precursor complexes, transition states, and products of $[CpPt(CO)]^+$. The heavy arrows indicate transition vectors for the single imaginary frequency. The MP2/LANL1DZ structures are shown in parentheses (see text).

frequencies, whereas in the MP2/LANL1DZ results both σ_{CH_2} and π_{CH_2} approaches can lead to the transition state possessing one imaginary frequency. When we examine the single imaginary frequency for each transition-state structure (see the heavy arrows in Figures 2−7), it is apparent that their transition vectors all are in accordance with the insertion process, primarily C−H bond stretching with a hydrogen migrating to the metal center. It must be pointed out that such characteristic three-centered cyclic transition states are consistent with mechanisms postulated by Bergman et al.[2a] and Jones et al.[2c] Furthermore, since both $[CpPd(CO)]^+$ and $[CpPt(CO)]^+$complexes have a cationic nature, one may argue the possibility of the four-center adduct mechanism, which has been observed for early transition metals.[16] All attempts to find a four-center adduct or transition state failed in both MP2/LANL1DZ and B3LYP/LANL2DZ calculations, so it is certain that the four-center adduct mechanism does not exist at the present levels of theory.

However, there are a few comments which can be made about Figures 2−7 and Table 1 that would be of interest to theoreticians. First, all attempts to find the triplet CpM(CO) (M = Ru^-, Os^-, Pd^+, Pt^+) complexes at the MP2/LANL1DZ level were unsuccessful since the maximum/RMS internal coordinate forces (<0.000 45/0.000 30 au, respectively) cannot be converged. This is presumably because the MP2 wave functions are based on the Hartree−Fock (HF) wave function; the MP2 wave function may be in serious error if the HF wave function has an internal instability. Nevertheless, our study

(16) (a) Watsen, P. L. *J. Am. Chem. Soc.* **1983**, *105*, 6491. (b) Watsen, P. L.; Parshall, G. W. *Acc. Chem. Res.* **1985**, *18*, 51. (c) Fendrick, C. M.; Marks, T. J. *J. Am. Chem. Soc.* **1984**, *106*, 425.

Table 1. Energies for Singlet and Triplet CpML Fragments and for the Process CH_4 + CpML → Precursor Complex → Transition State → Product[a]

system		singlet energy (hartrees)	ΔE_{st}[b] (kcal/mol)	reactant energy[c] (hartrees)	ΔE_{int}[d] (kcal/mol)	ΔE_{act}[e] (kcal/mol)	ΔH[d] (kcal/mol)
$CpRu(CO)^-$	MP2	−321.99699	*f*	−362.27614	−13.2	+3.28 (+4.01)	−30.2
	MP4SDTQ	−322.07715		−362.37485	−14.0	+4.59 (+5.44)	−26.1
	B3LYP	−400.71041	−11.7	−441.22489	−6.87	+3.24 (+4.00)	−27.2
$CpOs(CO)^-$	MP2	−320.67241	*f*	−360.95156	−19.4	+1.75 (+2.90)	−50.4
	MP4SDTQ	−320.74898		−361.04669	−18.2	+2.74 (+3.51)	−46.7
	B3LYP	−397.85012	−14.4	−438.36459	−10.1	+0.62 (+1.43)	−49.1
CpRh(CO)	MP2	−327.79797	+5.63	−368.07712	−13.6	+23.5 (+25.1)	−19.2
	MP4SDTQ	−327.87469	+9.71	−368.17239	−13.8	+10.4 (+11.4)	−13.3
	B3LYP	−416.31084	+0.11	−456.83208	−6.37	+12.9 (+13.8)	−4.24
CpIr(CO)	MP2	−325.76092	−7.28	−366.04007	−16.4	+15.5 (+16.5)	−32.8
	MP4SDTQ	−325.83587	−3.74	−366.13357	−15.8	+7.06 (+7.35)	−27.8
	B3LYP	−411.48311	−3.58	−451.99759	−9.64	+1.91 (+2.20)	−31.8
$CpPd(CO)^+$	MP2	−334.53728	*f*	−374.81643	−16.2	+28.4 (+29.5)	+9.06
	MP4SDTQ	−334.60476		−374.90246	−15.0	+29.3 (+30.4)	+13.2
	B3LYP	−433.26482	+1.03	−473.77930	−9.96	+29.4 (+30.6)	+19.3
$CpPt(CO)^+$	MP2	−331.62380	*f*	−371.90295	−17.4	+17.5 (+17.9)	−11.5
	MP4SDTQ	−331.69470		−371.99240	−16.5	+18.3 (+18.7)	−7.20
	B3LYP	−425.67850	+3.26	−466.19298	−10.9	+14.5 (+15.1)	−6.30

[a] At the MP2/LANL1DZ, MP4SDTQ//MP2/LANL1DZ, and B3LYP/LANL2DZ levels, respectively. [b] The energy relative to the corresponding singlet state. A negative value means that the triplet is the ground state. [c] The total energy of CH_4 at the MP2/LANL1DZ, MP4SDTQ//MP2/LANL1DZ, and B3LYP/LANL2DZ levels of theory are −40.279 15, −40.297 70, and −40.514 48 hartrees, respectively. [d] The energy relative to the corresponding reactants. [e] The energy relative to the corresponding precursor complex. The σ attack and π attack (in parentheses) are shown here (see text). [f] The triplet CpM(CO) (M = Ru^-, Os^-, Pd^+, Pt^+) cannot be found at the MP2/LANL1DZ level of theory.

shows that the DFT method (B3LYP/LANL2DZ) is able to avoid the problems that the ab initio method (MP2/LANL1DZ) has for calculating those triplet charged CpM(CO) complexes. This is further supported by the observation by Hertwig and Koch that DFT is more robust and less basis set sensitive than MP2 computations on molecules that normally are multireference problems in ab initio theory.[17]

Second, as mentioned above, only one transition structure (σ_{CH_2}) was found at the B3LYP/LANL2DZ level, whereas two transition structures (both σ_{CH_2} and π_{CH_2}) were found at the MP2/LANL1DZ level. The inconsistency between those two levels of theory may highlight the need for caution in the study of such processes. As suggested previously,[18] if at least two possible transition structures lie very closely in energy (near degenerate), more than one method should be employed to ensure consistency.

Third, in a comparison of the calculated geometries based on MP2 and B3LYP methods as shown in Figures 2−7, the B3LYP theory appeared to perform well, producing bond lengths marginally longer than those determined at the MP2 level. Also, comparing the B3LYP relative energies with MP2 and MP4SDTQ data as given in Table 1 reveals mixed results. The MP2 and MP4SDTQ stabilization energies (ΔE_{int}) of the precursor complexes are twice as large as the B3LYP results. Additionally, both MP2 and MP4SDTQ calculated activation energies (ΔE_{act}) for most cases are large when compared to B3LYP, while only the MP*n* and B3LYP barrier heights of $[CpPd(CO)]^+$ are in close agreement when compared to each other. However, the MP4SDTQ reaction enthalpies (ΔH) of the CpM(CO) (M = Ru^-, Os^-, Ir) systems are lower those of B3LYP by 1−4 kcal/mol, whereas MP4SDTQ reaction enthalpies of the CpM(CO) (M = Rh, Pd^+, Pt^+) cases are larger than B3LYP values by 1−9 kcal/mol. From these comparisons, it is certain that calculations using the MP2/LANL1DZ level of theory tend to result in shorter bonds and overestimate the correlation energies. The reason for this is presumably due to the absence of nodes in the valence orbitals of the LANL1DZ basis sets and the multireference problems in the MP2 theory. However, acceptable results may be obtained by optimizing the geometry of a structure at the MP2 level and calculating the energy at MP4SDTQ or higher levels of theory.[3e] Nevertheless, some of the corresponding results between MP*n* and B3LYP relative energies as shown in Table 1 could be fortuitous, and more work is needed to reach conclusions regarding any general trends.

Since the qualitative features of the potential energy profiles of the MP4SDTQ and B3LYP levels of theory are quite similar to each other, the use of the former will be essentially enough to provide qualitatively correct results. Accordingly, for the CpM(CO) (M = Ru^-, Os^-, Rh, Ir, Pd^+, Pt^+) complexes, the processes presented in Figures 2−7, respectively, can be examined and the resulting potential energy profiles are shown in Figure 8.

Some interesting conclusions can therefore be drawn from Figure 8. First, it can be clearly seen that, from both kinetic and thermodynamic viewpoints, the oxidative-addition reactions of the electron-rich systems (such as Ru^- and Os^-) are much more favorable than those of the electron-deficient systems (such as Pd^+ and Pt^+). For instance, the activation barriers from the precursor complex to the transition state at the present MP4SDTQ level of theory increase in the order Os^- (2.74 kcal/mol) < Ru^- (4.59 kcal/mol) < Ir (7.06 kcal/mol) < Rh (10.4 kcal/mol) < Pt^+ (18.3 kcal/mol) < Pd^+ (29.3 kcal/mol). Likewise, the reaction enthalpies decrease in the order Pd^+ (13.2 kcal/mol) > Pt^+ (−7.20 kcal/mol) > Rh (−13.3 kcal/mol) > Ru^- (−26.1 kcal/mol) > Ir (−27.8 kcal/mol) > Os^- (−46.7 kcal/mol). In other words, the electron density at the reacting metal center must play an important role in the C−H oxidative additions since it has been shown that an electron-rich metal center can

(17) Hertwig, R. H.; Koch, W. *J. Comput. Chem.* **1995**, *16*, 576.
(18) Frankcombe, K. E.; Cavell, K. J.; Yates, B. F.; Knott, R. B. *J. Phys. Chem.* **1996**, *100*, 18363.

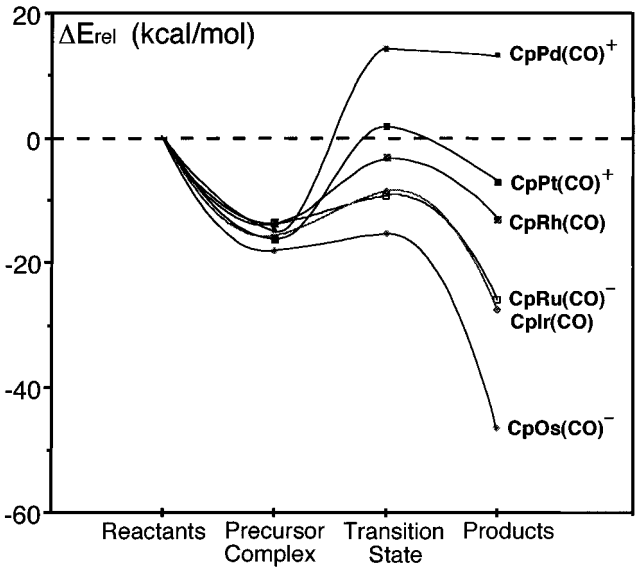

Figure 8. Potential energy profiles of the reaction of CpM(CO) (M = Ru, Os^-, Rh, Ir, Pd^+, Pt^+) with CH_4. All of the energies were calculated at the MP4SDTQ//MP2/LANL1DZ level.

result in a lower activation energy as well as a higher exothermicity for the C−H activation of methane. This theoretical finding is in accordance with the conventional concept mentioned by Bergman et al.[2b,d] and Jones et al.[2c]

Second, Figure 8 shows that the stabilization energies of the precursor complex relative to its corresponding reactant are comparable to one another among the d^8-CpM(CO) systems: i.e., Ru^- (−14.0 kcal/mol), Os^- (−18.2 kcal/mol), Rh (−13.8 kcal/mol), Ir (−15.8 kcal/mol), Pd^+ (−15.0 kcal/mol), and Pt^+ (−16.5 kcal/mol). Moreover, in the Pd^+ and Pt^+ cases, the energy of the transition state is apparently higher than that of the reactants, while in the other cases the energy of the transition state is below the energy of the reactants, as shown in Figure 8. This makes it easier for the latter cases to overcome the intrinsic barrier to activation of the C−H bond of alkanes. In other words, the CpM(CO) (M = Ru^-, Os^-, Ir) intermediates may readily undergo insertion into the saturated C−H bonds in a concerted fashion, whereas for Pd and Pt homologues, the process is significantly more difficult.

Third, considering the reverse process, i.e., reductive elimination from the alkyl hydride for the CpM(CO) species (right to left in Figure 8), it is apparent that the barrier to reductive elimination for the electron-deficient systems (such as Pd^+ and Pt^+) is much lower in energy than that for the electron-rich systems (such as Ru^- and Os^-). For example, the barrier energies increase in the order Pd^+ (1.04 kcal/mol) < Pt^+ (9.02 kcal/mol) < Rh (10.0 kcal/mol) < Ru^- (16.6 kcal/mol) < Ir (19.1 kcal/mol) < Os^- (31.2 kcal/mol). It is therefore predicted that the decreased electron density at the reacting metal center should also play a key role in the C−H bond-forming reductive-elimination reactions.

Fourth, our model calculations also suggest that the oxidative additions of the third-row transition metals would be preferable to those of the second-row transition metals, since it has been demonstrated not only that the former are thermodynamically favorable but also that the kinetic barriers associated with them are typically small. For instance, as seen in Figure 8, the facile oxidative addition is in the order Os^- > Ru^-, Ir > Rh, and Pt^+ > Pd^+. However, the reductive elimination of the second-row metals is more favorable than that of the third-row homologues. To our knowledge, the experimental supporting evidence comes from the fact that, in comparisons of oxidative additions of the iridium and rhodium intermediates to alkane C−H bonds, the products formed in the latter case are much less stable and undergo reductive elimination at −20 °C.[2b,d]

In summary, with the above results in hand, we are confident in predicting that *for the 16-electron CpM(CO) systems a more electron-rich as well as heavier transition-metal center (i.e., the third row) will facilitate the oxidative-addition reactions with alkane C−H bonds. In contrast, a very electron-deficient as well as lighter transition metal center (i.e., the second row) will tend to undergo reductive elimination reactions of C−H bond forming.* Besides the nature of the transition metals, the ligand effect, which can modulate the electron density at the reacting metal center, will also play a dominant role in the activation of C−H bonds of alkanes.[19] We encourage experimentalists to devise additional test cases to examine our predictions.

Acknowledgment. We are very thankful to the National Center for High-Performance Computing of Taiwan and the Computing Center at Tsing Hua University for generous amounts of computing time. We also thank the National Science Council of Taiwan for their financial support. We are also grateful to reviewers for critical comments and helpful corrections of the manuscript.

OM960837W

(19) For the study of ligand effects for oxidative additions, see: Su, M.-D.; Chu, S.-Y., manuscript in preparation.